Heliyon 10 (2024) e31227

Contents lists available at ScienceDirect

Heliyon

journal homepage: www.cell.com/heliyon

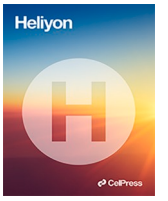

Research article

Conditional knockout mouse model reveals a critical role of peroxiredoxin 1 in oral leukoplakia carcinogenesis

Lingyu Li [a,1], Jing Li [b,1], Yunping Lu [c], Wenjing Li [b], Jing Yang [b], Min Wang [b], Congcong Miao [b], Zhenchuan Tian [b], Min Zhang [b], Xiaofei Tang [b,*]

[a] Department of Oral Pathology, Beijing Stomatological Hospital & School of Stomatology, Capital Medical University, Beijing, China
[b] Division of Oral Pathology, Beijing Institute of Dental Research, Beijing Stomatological Hospital & School of Stomatology, Capital Medical University, Beijing, China
[c] Department of Prosthodontics, Beijing Stomatological Hospital & School of Stomatology, Capital Medical University, Beijing, China

ARTICLE INFO

Keywords:
Peroxiredoxin 1
Oral leukoplakia
CRISPR-Cas systems
Gene knockout technique

ABSTRACT

Peroxiredoxin 1 (Prx1) is an antioxidant protein that may promote the carcinogenesis in oral leukoplakia (OLK). To investigate the effect of Prx1 on the oral mucosal epithelium of OLK, we generated a Prx1 conditional knockout (cKO) mouse model. The mRNA and gRNA were generated using the clustered regularly interspaced short palindromic repeats/CRISPR-associated protein 9 (CRISPR/Cas9) technique. An infusion cloning method was used to construct a homologous recombination vector. To obtain the F0 generation mice, fertilized eggs of C57BL/6J mice were microinjected with Cas9 mRNA, gRNA, and a donor vector. Polymerase chain reaction (PCR) amplification and sequencing were used to identify F1 generation mice. Using the cyclization recombination-enzyme-locus of the X-overP1 (Cre-loxP) system, we created a Prx1 cKO mouse model, and the effectiveness of the knockout was confirmed through immunohistochemistry. We examined the influence of Prx1 knockout on the occurrence of OLK in mice by constructing a model of tongue mucosa carcinogenesis induced by 4-nitroquinoline-1-oxide (4NQO). Prx1 modification was present in the F1 generation, as evidenced by PCR amplification and sequencing. $Prx1^{flox/flox}$: Cre + mice exhibited normal growth and fertility. Immunohistochemical analysis revealed that tongue epithelial cells in $Prx1^{flox/flox}$: Cre + mice displayed a distinct deletion of Prx1. An examination of the heart, liver, spleen, lung, and kidney tissues revealed no visible histological changes. Histological analysis showed a reduction in the occurrence of the malignant transformation of OLK in the tongue tissues of $Prx1^{flox/flox}$: Cre + mice. Ki67 immunostaining showed that Prx1 knockout significantly inhibited cell proliferation in the tongue epithelial. Our research developed a conditional knockout mouse model for Prx1. The obtained results provide insights into the function of Prx1 in the development of oral cancer and emphasize its potential as a therapeutic target for precancerous oral lesions.

1. Introduction

Peroxiredoxin 1 (Prx1) is an essential antioxidant enzyme that plays a crucial role in maintaining redox homeostasis. It is

* Corresponding author. No.4 Tiantan Xili, Dongcheng District, Beijing, 100050, China.
E-mail address: xftang10@ccmu.edu.cn (X. Tang).
[1] These authors contributed equally to this study.

https://doi.org/10.1016/j.heliyon.2024.e31227
Received 9 January 2024; Received in revised form 12 April 2024; Accepted 13 May 2024
Available online 17 May 2024

predominantly localized in the cytoplasm of mammalian cells and widely expressed in diverse tissues and organs [1]. Research has indicated that Prx1 levels are increased in malignant conditions, such as oral, esophageal, lung, and colorectal cancers [2,3]. Moreover, it is closely associated with tumor cell proliferation, apoptosis, senescence, invasion, metastasis, and prognosis [2,3]. In our previous study, we found a notable rise in the levels of Prx1 in head and neck squamous cell carcinoma (HNSCC) by analyzing the Cancer Genome Atlas program database. Furthermore, we observed a strong correlation between high Prx1 expression and clinical staging, tumor histological grading, and patient prognosis [4]. Similarly, we observed a significant rise in the expression of Prx1 in oral leukoplakia (OLK). Whether Prx1 is important in the malignant transformation of OLK remains unknown, and the mechanism associated remains unclear.

In previous studies, we have found that nicotine may promote the development of oral precancerous lesions by Prx1 and its binding proteins [5–7], and prx1 may play a crucial role in the initiation and progression of OLK by regulating the mitogen-activated protein kinase signaling pathway and suppressing apoptosis [7,8]. However, these studies were performed in vitro, as well as in vivo in $Prx1^{+/-}$ mice. $Prx1^{-/-}$ mouse embryos display an embryonic-lethal phenotype and they were difficult to obtain by crossing the $prx1^{+/-}$ mice. With the cyclization recombination-enzyme-locus of the X-overP1 (Cre-loxP) conditional knockout technique, it is possible to circumvent the embryonic lethal phenotype of conventional Prx1 knockout mice.

In the present study, we constructed a Prx1 conditional knockout (cKO) mouse. Using this novel animal model, we investigated the role of Prx1 in OLK carcinogenesis. We found that the Prx1 cKO in the oral mucosa epithelia inhibited cell proliferation and caused a substantial decrease in the incidence of oral cancer. The findings of the present will facilitate future research focusing on the development of therapies targeting Prx1 to prevent and treat precancerous lesions.

2. Materials and methods

2.1. Generation of Prx1 cKO mouse model

Using the Cre-loxP system, we generated a Prx1 cKO mouse model. The C57BL/6J-$Prx1^{flox/+}$ (F1 generation mice) were designed and provided by the Shanghai Model Organisms Center, and KRT14-cre (K14-Cre) mice (JAX stock #004782) were procured from Jackson Laboratory [9]. Subsequently, homologous recombination was used to modify the Prx1 gene. Briefly, clustered regularly interspaced short palindromic repeats (CRISPR)-associated protein 9 (Cas9) mRNA was obtained through in vitro transcription with mMESSAGE mMACHINE T7 Ultra Kit (Ambion, USA) according to the manufacturer's instructions (Fig. 1A). Two gRNAs targeted to delete exon 3 were in vitro transcribed using the MEGAshortscript Kit (ThermoFisher, USA). The gRNAs sequence (5′-3′) were TCAGGGTGAGATCCAGTAGCAGG and TTAATGTATAATAAGTCTTTGGG. The infusion cloning method was used to construct a donor vector for homologous recombination. The donor vector consisted of a 5′ homologous arm measuring 3.0 kb, a flox region measuring 0.9 kb, and a 3′ homologous arm measuring 3.0 kb (Fig. 1B). The 5′ and 3′ homologous arms were designed to flank the flox region, which was the target site for modification (Fig. 2). To obtain F0 generation mice, the fertilized eggs of C57BL/6J mice were injected with Cas9 mRNA, gRNA, or a donor vector. Polymerase chain reaction (PCR) amplification was used to identify positive F0 mice, which were then bred with C57BL/6J mice to produce positive F1 mice. The positive F1 mice were identified using PCR amplification and sequencing. Homozygous knockout $Prx1^{flox/flox}$ mice were obtained by selfing F1 mice. To eliminate Prx1 from tongue epithelial cells, $Prx1^{flox/flox}$ mice were bred with K14-Cre mice to generate $Prx1^{flox/flox}$: Cre + mice (Fig. 3).

2.2. OLK carcinogenesis induction and sample collection

The animal experiments conducted herein were approved by the Ethics Committee of the Beijing Stomatological Hospital (No.

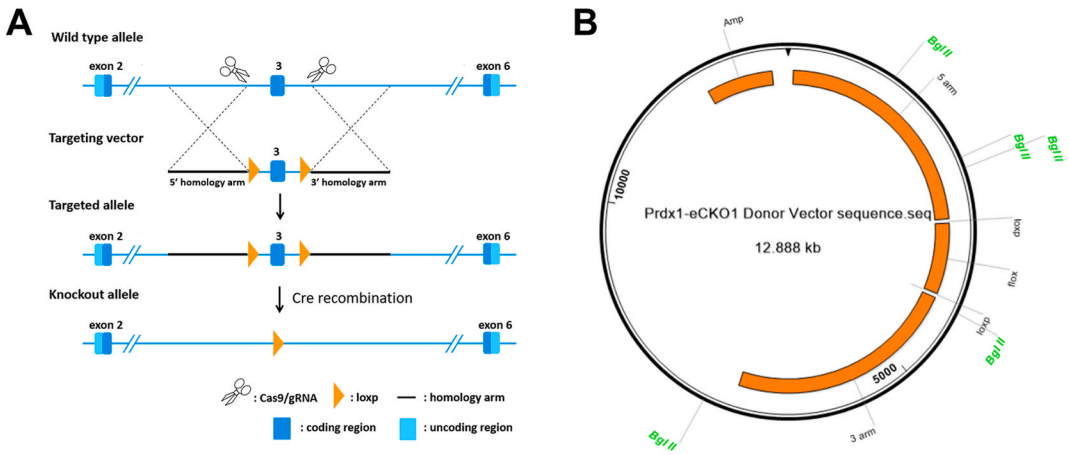

Fig. 1. Schematic diagram of Prx1 conditional knockout mouse construction. (A) Schematic diagram of Prx1 gene modification. (B) Schematic diagram of homologous recombination plasmid.

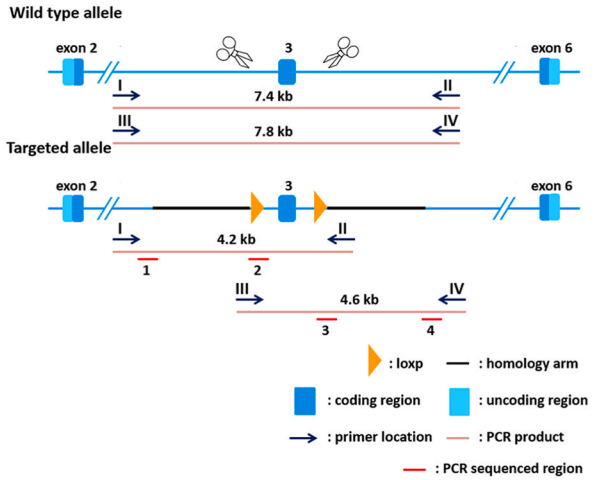

Fig. 2. Schematic diagram of identification strategy for F0 and F1 generation mice.

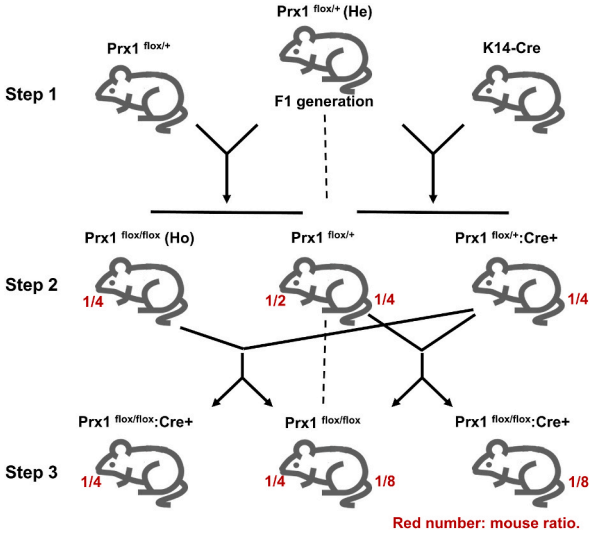

Fig. 3. Schematic diagram of mating.

KQYY-202202-003) in conformance with the ARRIVE guidelines. This present study involved a group of 40 mice, aged between 6 and 8 weeks, with a weight range of 16–20 g. Each group consisted of 20 cKO mice ($Prx1^{flox/flox}$: Cre+) and 20 control mice ($Prx1^{flox/flox}$). The study was divided into four categories according to the usage of 4-nitroquinoline 1-oxide (4NQO), with ten mice in the $Prx1^{flox/flox}$ group and ten mice in the $Prx1^{flox/flox}$: Cre + group fed with a regular diet. The 4NQO + $Prx1^{flox/flox}$ group consisted of ten control mice, whereas the 4NQO + $Prx1^{flox/flox}$: Cre + group comprised ten cKO mice. The 4NQO + $Prx1^{flox/flox}$ group and 4NQO + $Prx1^{flox/flox}$: Cre + group were administered a dosage of 100 mg/kg of the 4NQO solution for 12 weeks. After 12 weeks, the 4NQO solution was replaced with purified water. All mice were weighed every two weeks. After 24 weeks, the mice were euthanized and their tongues, hearts, livers, spleens, lungs, and kidneys were collected for histological examination.

2.3. PCR analysis

DNA was extracted from mouse tongue tissues using the alkali lysis method. Polymerase chain reaction was performed using the extracted DNA as a template. Briefly, the PCR reaction mixture consisted of 2 μL specific paired primers for amplification, 10 μL 2 × Taq PCR StarMix (Dye) (GeneStar, China), 4 μL of DNA template, and 2 μL sterile water. Amplification products were analyzed by electrophoresis on 1.5 % agarose gels and visualized by using GelRed staining. Genotype identification of F0 and F1 generation mice was performed by PCR amplification using primers I, II, III, and IV. Genotype identification strategies for F0 and F1 mice are shown in Fig. 3. The X-overP1 (loxP) locus was detected by PCR amplification using primers P1 and P2. The K14-Cre transgene was detected by PCR amplification using the primers P5 and P6. The primer sequences used in the present study are listed in Table 1.

2.4. Sanger sequencing

The sequencing reaction mixture was prepared by combining the PCR product, DNA polymerase, primers, and fluorescently labelled dNTPs. Sanger sequencing was performed using an automated DNA sequencing system. Electropherogram data generated by the sequencer were used for subsequent analysis. The obtained DNA sequence was compared with known reference sequences to identify variations.

2.5. Hematoxylin and eosin staining

To observe the morphology of the tongue, heart, liver, spleen, lungs, and kidneys tissues, tissue slices of tissues were prepared as described previously and stained with hematoxylin and eosin. Briefly, the sections were dewaxed thrice in xylene for 10 min. The sections were soaked in 100 %, 95 %, or 75 % ethanol each for 5 min each. Finally, the sections were washed twice with purified water for 5 min each, and subsequently treated with hematoxylin for 8 min. After rinsing with distilled water, the samples were separated using 0.5 % ethanol hydrochloride and bluing with 0.5 % ammonia for 10 s. Then the sections were washed slowly with distilled water for 10 min and counterstained with for 1 min. Subsequently, the sections were subjected to two rounds of dehydration in 95 % ethanol for 5 min each, followed by two rounds in 100 % ethanol for 5 min each, and, finally, three rounds in xylene for 10 min each. Sealing was performed using resin containing neutral gum.

Hematoxylin and eosin-stained sections of mouse tongue tissue were observed and evaluated by professional pathologists under double-blind conditions. Tissue lesions were assessed according to the classification criteria provided by the WHO Health Organization (2017). The results were classified as follows: normal, mild dysplasia, moderate dysplasia, severe dysplasia, and oral squamous cell carcinoma (OSCC).

2.6. Immunohistochemistry

Immunohistochemistry was conducted to examine the expression of the Prx1 and Ki67 in tongue tissues. Briefly, the sections were dewaxed using xylene and gradient alcohol, and then the antigens were repaired using an ethylenediaminetetraacetic acid antigen buffer (Maixin, China). Thereafter, the sections were incubated with 3 % hydrogen peroxide for 15 min and 10 % goat serum (Nakasugi Jinqiao, China) for 30 min at 37 °C. Next, the sections were exposed to anti-Prx1 antibodies (Abcam, USA) and anti-Ki67 antibodies (Maixin, China), respectively. And the sections were incubated overnight at a temperature of 4 °C. Prx1 and Ki67 expression was detected by performing diaminobenzidine (Maixin, China) staining after incubation with the respective horseradish peroxidase.

2.7. Statistical analysis

GraphPad Prism 8.0 software was utilized for conducting all data analyses. The findings were presented as the average plus standard deviation. The data was analyzed using a one-way analysis of variance, and then Bonferroni's post hoc test was conducted for multiple comparisons. A P value below 0.05 was regarded as statistically significant.

3. Results

3.1. Homologous recombination plasmid digestion identification

Digestion of the homologous recombinant vector was performed using linearized electrophoresis. The BgIII digestion identification revealed band sizes of 6727 bp, 3261 bp, 1630 bp, and 1147 bp, which matched the theoretical band sizes. A theoretical band of 123 bp was not observed, possibly because of low product yield (Fig. 4A).

3.2. Acquisition of homologous recombinant positive F0 and F1 generation mice

Homologous recombinant positive F0 and F1 mice were obtained using PCR amplification. The 5′ arm of the homologous recombinant-positive genomic DNA should yield a 4.2 kb fragment, while the negative genomic DNA should yield a 7.4 kb fragment.

Table 1
Primers used in the present study.

Primer	Sequence 5′-3′	Primer type
I	TCAGTTCTTGCTCGCTCTCATCAT	Forward
II	CAACCCACTATACCTAACTGC	Reverse
III	TGAACTCAAAGACATCCTC	Forward
IV	AAGCCTTAAAAACCCAAAATACAT	Reverse
P1	GGGGCATTGTTAGAGACTTTCACT	Forward
P2	ACTGTTTCTTCTTTGGTTTGCTAA	Reverse
P5	AACTTGTGATTTTCCTGCTTCT	Forward
P6	TATACCTTTAATCCTACCTACTCA	Reverse

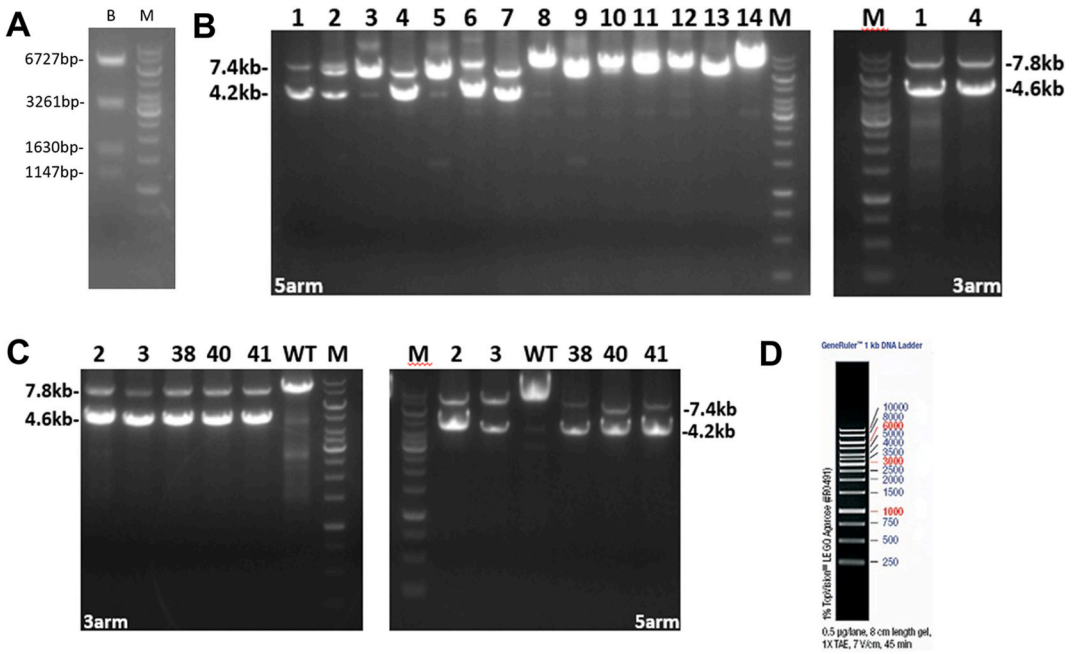

Fig. 4. Identification of homologous recombinant vector and F0 and F1 generation mice. (A) Identification of homologous recombinant vector through enzyme digestion and linearized electrophoresis image. (B) PCR identification electrophoresis image of homologous recombination positive F0 generation mice. (C) PCR identification electrophoresis image of homologous recombination positive-F1 generation mice. (D) GeneRulerTM 1 kb DNA Ladder. B: BgIII enzyme digestion identification result; Numbers: generation mouse numbers; M: 1 kb DNA marker.

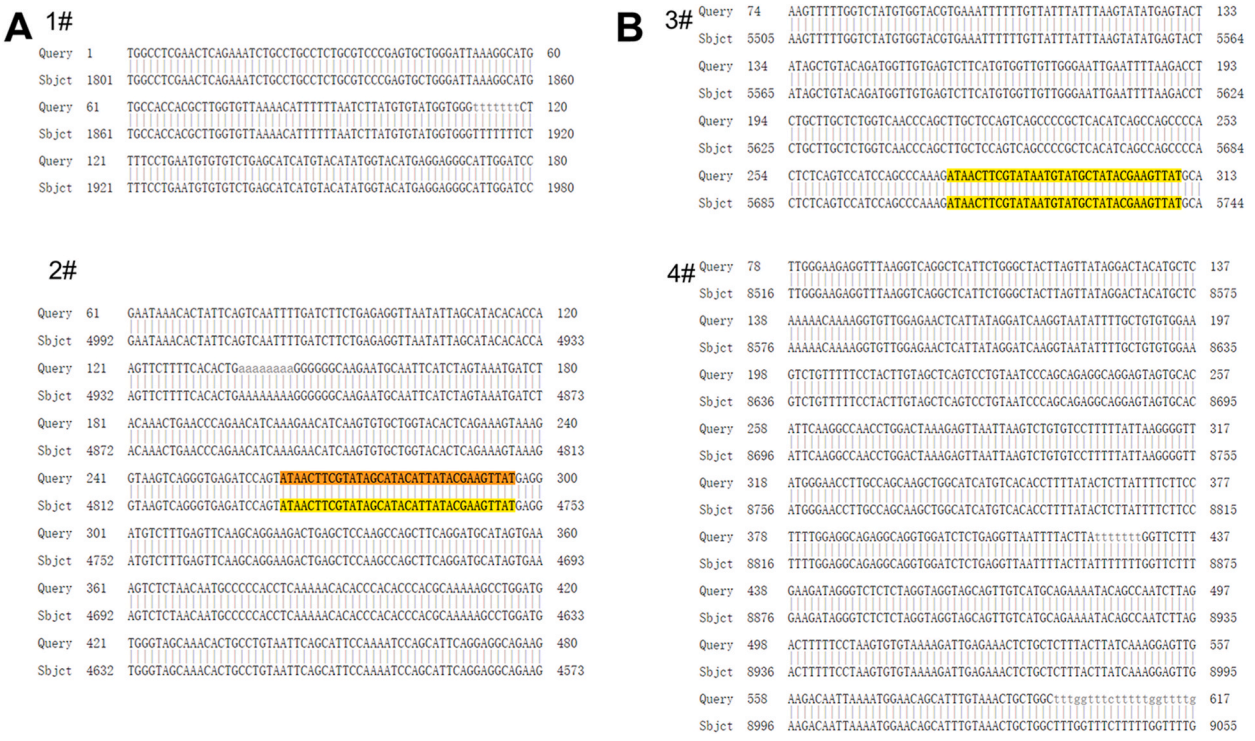

Fig. 5. PCR identification sequencing alignment results of F1 generation mice. (A) 5′ homologous arm identification was performed by sequencing two PCR products, labelled 1 and 2. (B) 3′ homologous arm identification was performed by sequencing two PCR products, labelled 3 and 4. Sbjct: the target sequence (Prdx1-eCKO1 Recombinated Genomic DNA sequence); Query: the sequencing result. Highlighted marks: the loxP sequence.

Similarly, the 3′ arm of the homologous recombinant-positive genomic DNA should yield a 4.6 kb fragment, and the negative genomic DNA should yield a 7.8 kb fragment. Mouse numbers 1 and 4, identified as F0 generation mice with positive double-arm homologous recombination, are shown in Fig. 4B via long-fragment PCR electrophoresis. The PCR electrophoresis results for the 5′ and 3′ arm PCR identification in the F1 generation mice are shown in Fig. 4C. Positive mice identified by PCR were mouse numbers 2, 3, 38, 40, and 41.

The PCR products of the F1 generation-positive mice were subjected to four sequencing reactions. In the sequencing results of No.2 sequencing reactions for the 5′ arm identification, the highlighted region corresponds to the loxP sequence. Similarly, in the sequencing results No.3 for the 3′ arm identification, the highlighted region corresponds to the loxP sequence (Fig. 5). These results indicated the successful filtering of homologous recombinant-positive F0 and F1 generation mice.

3.3. Acquisition of $Prx1^{flox/flox}$: Cre + mice

The $Prx1^{flox/flox}$: Cre + mice and their controls were generated by mating of mice using the approach depicted in Fig. 3. Table 2 provides the band sizes corresponding to the genotypes of the fetal mice by PCR, and the representative identification results are shown in Fig. 6AB. Genotype of No.2 was $Prx1^{flox/flox}$: Cre+, genotypes of No.5 and No.6 were $Prx1^{flox/+}$: Cre+, genotypes of No.3 and No.4 were $Prx1^{flox/flox}$, and the genotype of No.1 was wild type (WT). Immunohistochemical detection of Prx1 expression was performed in the tongue tissues of mice with genotypes $Prx1^{flox/flox}$ and $Prx1^{flox/flox}$: Cre+. The results showed that Prx1 expression was positive and exhibited a diffuse distribution in the tongue epithelium of mice with the $Prx1^{flox/flox}$ genotype. In contrast, the tongue epithelium of $Prx1^{flox/flox}$: Cre + mice showed no expression of Prx1, suggesting the successful construction of Prx1 cKO mice (Fig. 6C).

3.4. Prx1 knockout reduces the carcinogenesis rate of OLK

During the experiment, the trends in body weight changes in the mice were recorded. As shown in Fig. 7, except for the control group, in which the body weight of the mice remained relatively stable, the body weights of mice in the other groups showed an initial increase, followed by a decrease. After 12 weeks of 4NQO administration in drinking water, the body weights of mice in all groups started to decrease gradually as the tongue tissue lesions worsened. There were no significant differences in body weights between the groups ($P > 0.05$). We also carried out histological examination of the heart, liver, spleen, lung, and kidney from mice. No histological changes were observed for the heart, liver, spleen, lung, and kidney, for all groups (Fig. 8).

The tongue mucosa of 20 mice in the $Prx1^{flox/flox}$ group and $Prx1^{flox/flox}$ group: Cre+ was normal, while eight mice in the 4NQO + $Prx1^{flox/flox}$ group and six mice in 4NQO + $Prx1^{flox/flox}$ group: Cre + developed into carcinoma. These results suggested that Prx1 knockout of Prx1 may suppress the occurrence of OSCC (Fig. 9AB, Table 3). We evaluated the Ki67 positive cell rate to examine the proliferation in the tongue epithelium. It was manifested that the positive rate of Ki67 in the 4NQO + $Prx1^{flox/flox}$ group: Cre+ was significantly decreased compared to the 4NQO + $Prx1^{flox/flox}$ group ($P < 0.01$, Fig. 9CD).

4. Discussion

Human Prx1 gene is located on chromosome 1 (1p34.1) and is primarily found in the cytosol. However, it has also been observed in the nucleus, plasma membrane, and centrosome [10]. Prx1 functions as an antioxidant enzyme, controlling the levels of reactive oxygen species (ROS) within cells [11,12]. Under conditions of heightened oxidative stress, Prx1 undergoes structural change, resulting in the formation of a durable and condensed decameric structure. This structure serves as a molecular companion to control cellular growth and programmed cell death, while also preserving the cellular redox balance [2,13]. Studies have indicated that there is a significant level of Prx1 exhibits significant expression in different types of tumors, such as HNSCC [14], non-small-cell lung cancer [3], triple-negative breast cancer [15], esophageal cancer [16], CRC [4], and many others [17]. Prx1 is closely associated with tumor cell proliferation, apoptosis, senescence, invasion, metastasis, and prognosis [2]. Consistent with these findings, our research has demonstrated elevated expression of Prx1 in OSCC and OLK tissues and cells [8,18]. We also investigated the influence of nicotine, a known risk factor for oral cancer, on OSCC and found that nicotine stimulated an increase in ROS levels and enhanced Prx1 mRNA and protein expression [5,19]. These findings suggested that Prx1 plays a crucial role in the development and progression of oral cancer. However, the exact mechanisms by which Prx1 exerts its affects in OLK remain unclear, highlighting the significance of studying its function in detail.

In our previous study, we successfully generated $Prx1^{+/-}$ mice to investigate the molecular mechanism of Prx1 in OLK and OSCC,

Table 2
Location of genotype-specific primer bands.

Primer	Genotype	Location
P1、p2	WT	294 bp
	$Prx1^{flox/+}$	294 bp; 347 bp
	$Prx1^{flox/flox}$	347 bp
P5、P6	WT	1365 bp
	Cre-Cre+	1473 bp
		522 bp

WT: wild type.

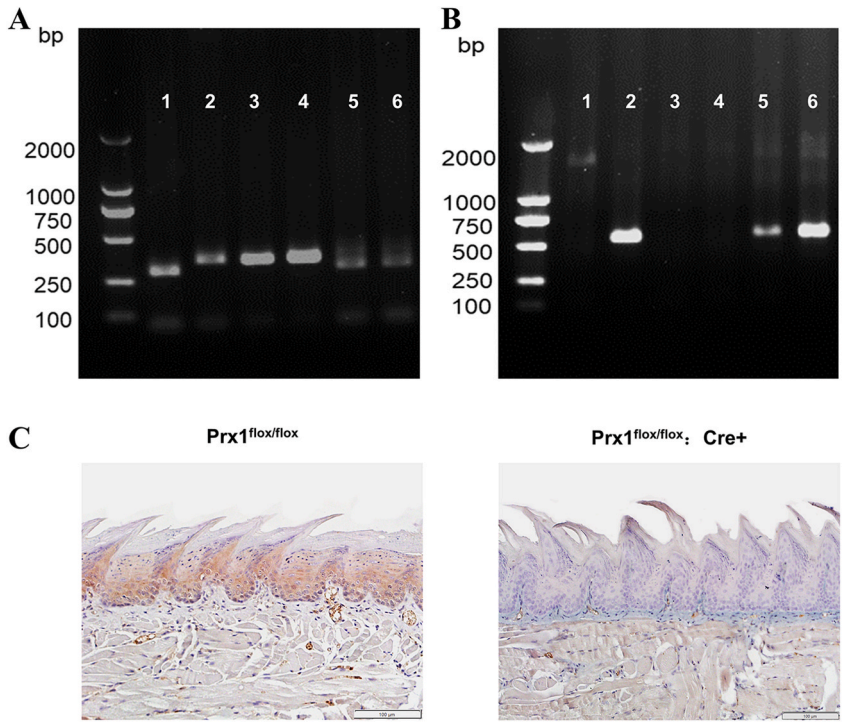

Fig. 6. Identification of Prx1 $^{flox/flox}$:Cre + mice. (A) To identify the Prx1 gene in mice. WT: one band of 294 bp; Heterozygous: two bands of 294 and 347 bp, respectively; Homozygous: one band of 347 bp. (B) Cre activity PCR identification conditions. With Cre activity: 522 bp; no Cre activity: 1473 bp; wild type: 1365 bp. (C) Immunohistochemical staining was used to detect the expression of Prx1 in mouse tongue mucosa.

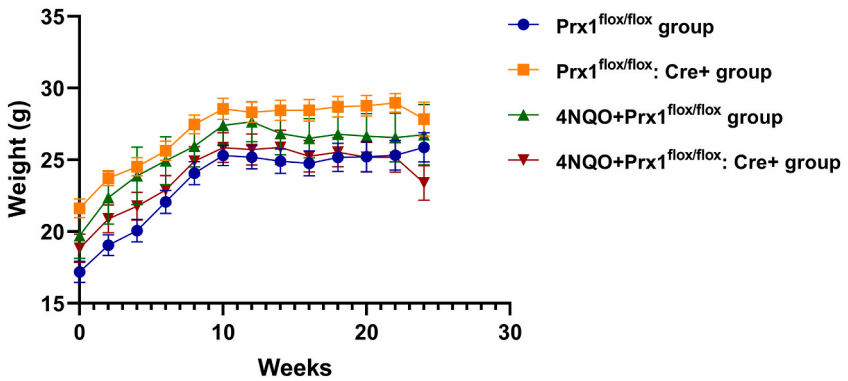

Fig. 7. Trend of body weight in each group.

and the findings revealed that Prx1 indeed promotes the progression of tongue precancerous lesions, as evidenced by increased cell apoptosis in Prx1$^{+/-}$ mouse tongue precancerous lesions [20]. However, whole-body Prx1 gene knockdown mice exhibited certain phenotypes, including premature aging, altered body composition (such as obesity), and coarse and oily fur, indicating systemic symptoms after Prx1 suppression. Neumann et al. revealed that Prx1 knockout mice displayed pronounced hemolytic anemia [21,22] and various malignant cancers, such as lymphomas, sarcomas, and carcinomas, leading to a reduced lifespan [23]. In different inflammation disease models, Prx1$^{-/-}$ shows conflicting results [24]. Prx1 enhances cerebral ischemia-reperfusion injury by activating inflammation and apoptosis [25], and it initiates inflammation in the ozone-exposed lungs [26]. Prx1 deficiency, however, aggravates pulmonary inflammation and fibrosis in a bleomycin-treated model [27]. Studies using Prx1-knockout mouse models have also shown that Prx1 is involved in the maintenance of stemness in mouse embryonic stem cells by suppressing ROS/JNK-induced neurogenesis [28], modulation of cellular senescence in mouse embryonic fibroblasts [29]. In contrast to traditional gene knockdown methods, cKO mice generated using CRISPR/Cas9 technology enable precise spatiotemporal control of gene expression, thus overcoming some of the limitations associated with systematic gene knockout, wherein essential genes may cause embryonic lethality. cKO mice offer a valuable tool in modern biological science, allowing for the selective targeting of gene knockouts in specific tissues or

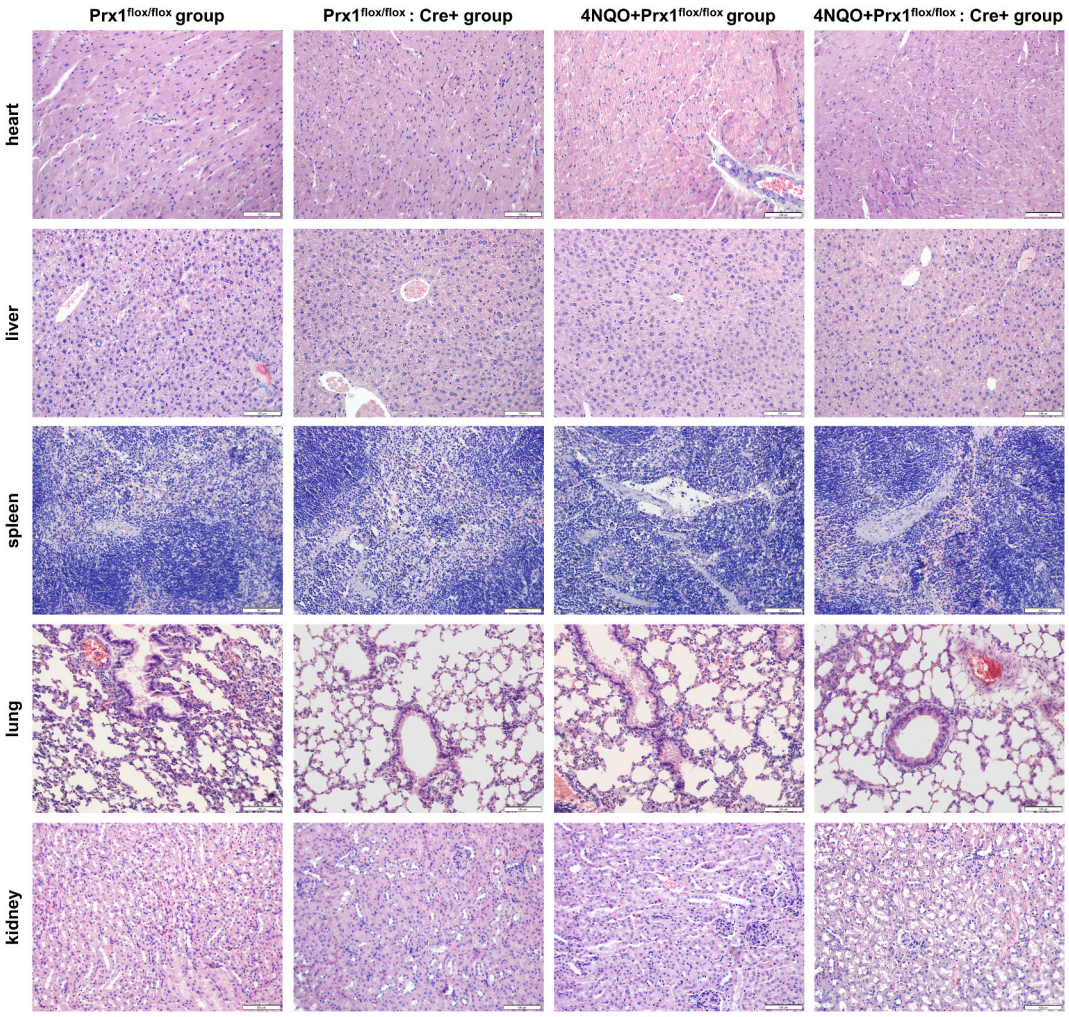

Fig. 8. Histopathological analysis of heart, liver, spleen, lung, and kidney in each group (200 × magnification).

at specific developmental stages, thereby enabling more accurate functional analysis of target genes.

To further understand of the role of Prx1 in OLK, it is imperative to develop a mouse model with conditional gene knockout of Prx1. In the present study, we employed CRISPR/Cas9 methodology to fabricate the Cas9 mRNA and gRNA. A homologous recombination vector was constructed using an infusion cloning method. To obtain the F0 generation mice, fertilized eggs of C57BL/6J mice were microinjected with Cas9 mRNA, gRNA, and a donor vector. PCR amplification and sequencing were used to identify the F1 generation mice with positive results. Using the Cre-loxP system, we successfully inserted loxP sequences flanking the Prx1 gene exon, leading to specific Prx1 gene knockout in the ectoderm of $Prx1^{flox/flox}$: Cre + mice.

The main objective of the present study was to investigate the role of Prx1 in the oral epithelium. To achieve this, we employed CRISPR/Cas9 technology and utilized K14-cre mice to selectively knock out the Prx1 gene within the tongue epithelium of mice. The utilization of different Cre mouse models allows for conditional gene knockout in specific tissues, facilitating the investigation of gene function in a tissue-specific context [30,31]. In K14-Cre mice, the Cre recombinase is produced by the regulation of the human K14 promoter [32]. The promoters of K14 and K5 in humans have proven to be valuable for directing transgene expression to the actively dividing basal layer of the mouse epidermis and the outer root sheath of the oral epithelia, hair follicles, and esophagus [33,34]. By inserting loxP sequences flanking the Prx1 gene exon, we were able to successfully create Prx1 knockout in the ectoderm and its derivatives, including the skin, dental epithelium, and oral ectoderm [9]. In the present study, $Prx1^{flox/flox}$: Cre + mice appeared healthy and fertile, developed normally, and had a normal life span. Immunohistochemical results showed that Prx1 expression was positive and exhibited a diffuse distribution in the tongue epithelial tissues of $Prx1^{flox/flox}$ mice. In contrast, no Prx1 expression was observed in the tongue epithelium of $Prx1^{flox/flox}$: Cre + mice, confirming the successful construction of Prx1 knockout mice.

To further investigate the influence of Prx1 on oral cancer using the cKO mouse model for Prx1, we used a mouse model induced by 4NQO, a potent carcinogen known to induce oral cancer in rodents. During the observational period, there was no difference in the growth of body weight and histological structure of major organs. Pathological examination of tongue tissues in each group revealed

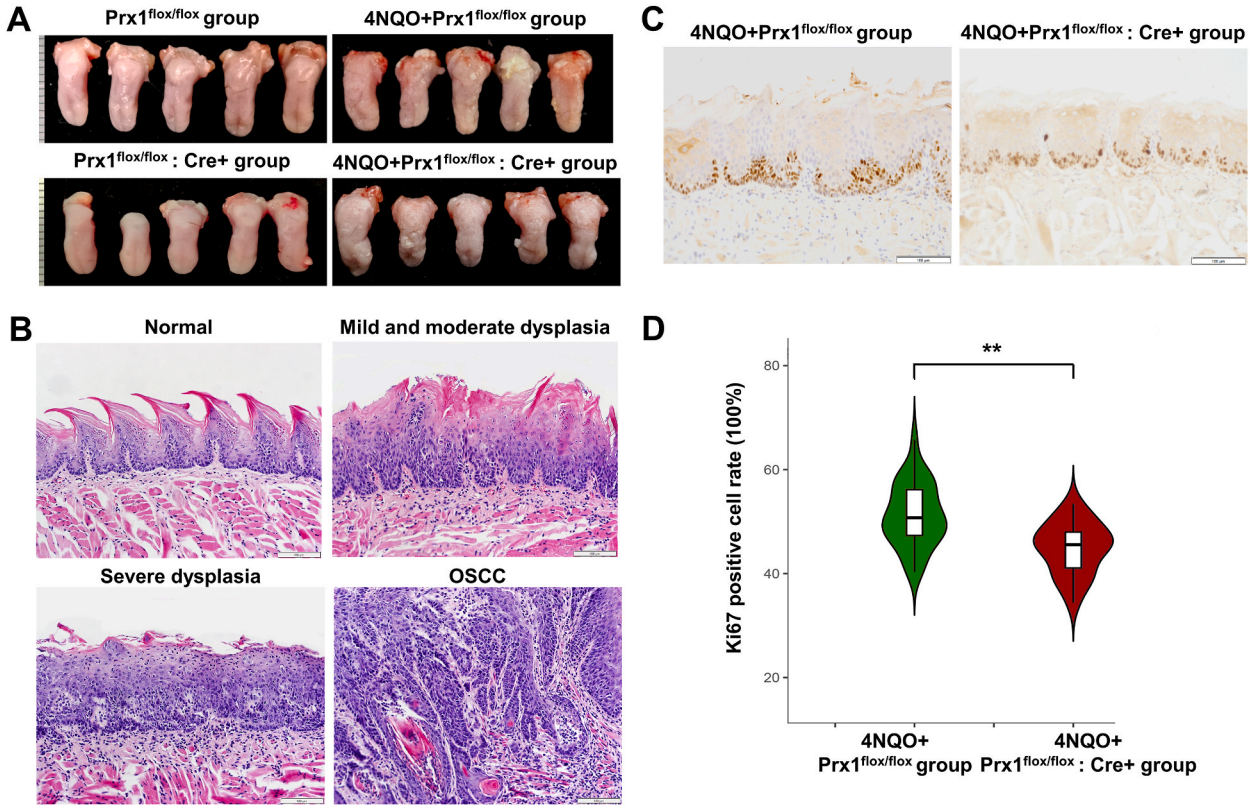

Fig. 9. Prx1 knockout reduces the carcinogenesis rate of OLK. (A) Macroscopic observation of mouse tongue tissue in each group. (B) Representative histopathological lesions of mouse tongue tissue (200 × magnification). (C) Immunohistochemistry staining of the proliferation marker Ki67 in each group (200 × magnification). (D) Violin plot of the positive rate of Ki67 in each group. $^{**}P < 0.01$.

Table 3
The pathological diagnostic results of mice in each group.

Groups	N	Normal	Mild and moderate dysplasia	Severe dysplasia	OSCC
$Prx1^{flox/flox}$ group	10	10	0	0	0
$Prx1^{flox/flox}$: Cre + group	10	10	0	0	0
4NQO + $Prx1^{flox/flox}$ group	10	0	1	1	8
4NQO + $Prx1^{flox/flox}$: Cre + group	10	0	3	1	6

OSCC: oral squamous cell carcinoma.

that Prx1 knockout reduced the progression of tongue precancerous lesions in mice and alleviated their severity. The protein Ki67 has been confirmed as a molecular marker for proliferating cells in OPMDs and OSCC [35]. Ki67 immunostaining showed that Prx1 knockout significantly inhibited the cell proliferation in the tongue epithelium. These findings indicate a potential role of Prx1 in promoting tongue cancer progression and support its significance as a target for intervention strategies.

The successful construction of the Prx1 cKO mouse model herein provides a solid foundation for future investigations into the functional role of the Prx1 gene and its correlation with oral precancerous lesions occurrence, and development. Whole-body Prx1 gene knockdown affects lifespan, Prx1 cKO mouse allows for the study of the long-term effects of postnatal loss of Prx1, as well as the role of tissue-specific loss of this gene during development. However, potential limitations of Prx1 cKO may require a longer observation period in experiments. Further studies using this mouse model will shed light on the underlying mechanisms by which Prx1 contributes to OLK progression, potentially unveiling new therapeutic targets and strategies for disease management.

5. Ethics declarations

All animal experiments in this study were performed under the guidelines and with the approval of the Ethical Committee of the Beijing Stomatological Hospital (No. KQYY-202202-003).

Data availability statement

Data are available on reasonable request.

CRediT authorship contribution statement

Lingyu Li: Writing – review & editing, Writing – original draft, Methodology, Formal analysis, Conceptualization. **Jing Li:** Writing – review & editing, Writing – original draft, Methodology, Formal analysis, Data curation. **Yunping Lu:** Writing – original draft, Methodology, Data curation. **Wenjing Li:** Writing – original draft, Data curation. **Jing Yang:** Writing – original draft, Methodology, Data curation. **Min Wang:** Writing – original draft, Methodology, Data curation. **Congcong Miao:** Writing – original draft, Formal analysis. **Zhenchuan Tian:** Writing – original draft, Methodology, Formal analysis. **Min Zhang:** Writing – review & editing, Supervision, Project administration, Methodology, Conceptualization. **Xiaofei Tang:** Writing – review & editing, Supervision, Project administration, Funding acquisition, Conceptualization.

Declaration of competing interest

No potential conflict of interest was reported by the authors.

Acknowledgments

The present study was supported by the National Natural Science Foundation of China (No.82270977).

References

[1] H.A. Woo, S.H. Yim, D.H. Shin, D. Kang, D.Y. Yu, S.G. Rhee, Inactivation of peroxiredoxin I by phosphorylation allows localized H(2)O(2) accumulation for cell signaling, Cell 140 (4) (2010) 517–528, https://doi.org/10.1016/j.cell.2010.01.009.
[2] C. Ding, X. Fan, G. Wu, Peroxiredoxin 1 - an antioxidant enzyme in cancer, J. Cell Mol. Med. 21 (1) (2017) 193–202, https://doi.org/10.1111/jcmm.12955.
[3] C. Song, G. Xiong, S. Yang, X. Wei, X. Ye, W. Huang, et al., PRDX1 stimulates non-small-cell lung carcinoma to proliferate via the Wnt/beta-Catenin signaling, Panminerva Med. 65 (1) (2023) 37–42, https://doi.org/10.23736/S0031-0808.20.03978-6.
[4] L.Y. Li L, Y. Shen, S. Liang, W. Wang, M. Zhang, M. Wang, X. Tang, Expression of Prx1 and its clinical significance in the patients with head and neck squamous cell carcinoma: analysis based on the data mining of TCGA Beijing Journal of Stomatology 30 (1) (2022) 6–10.
[5] M. Qi, L. Li, Y. Lu, H. Chen, M. Zhang, M. Wang, et al., Proteome profiling to identify peroxiredoxin 1 interacting protein partners in nicotine-associated oral leukoplakia, Arch. Oral Biol. 108 (2019) 104537, https://doi.org/10.1016/j.archoralbio.2019.104537.
[6] M. Qi, H. Chen, L. Wang, M. Zhang, X. Tang, Interaction between transcriptional factor E26 transformation specific 1 and peroxiredoxin 1 innicotine-induced oral precancerous lesion cells, Chin. J. Stomatol. 52 (12) (2017) 729–734, https://doi.org/10.3760/cma.j.issn.1002-0098.2017.12.004.
[7] J.X. Li L, H. Chen, M. Qi, Y. Lu, J. Yang, M. Wang, X. Tang, Tobacco inhibits apoptosis by regulating Prx1/Ets1 binding in oral leukoplakia, Beijing Journal of Stomatology 28 (2) (2020) 61–66.
[8] C. Wang, W. Niu, H. Chen, N. Shi, D. He, M. Zhang, et al., Nicotine suppresses apoptosis by regulating alpha7nAChR/Prx1 axis in oral precancerous lesions, Oncotarget 8 (43) (2017) 75065–75075, https://doi.org/10.18632/oncotarget.20506.
[9] H.R. Dassule, P. Lewis, M. Bei, R. Maas, A.P. McMahon, Sonic hedgehog regulates growth and morphogenesis of the tooth, Development 127 (22) (2000) 4775–4785, https://doi.org/10.1242/dev.127.22.4775.
[10] H. Shau, A. Kim, Identification of natural killer enhancing factor as a major antioxidant in human red blood cells, Biochem. Biophys. Res. Commun. 199 (1) (1994) 83–88, https://doi.org/10.1006/bbrc.1994.1197.
[11] C.C. Sun, W.R. Dong, T. Shao, J.Y. Li, J. Zhao, L. Nie, et al., Peroxiredoxin 1 (Prx1) is a dual-function enzyme by possessing Cys-independent catalase-like activity, Biochem. J. 474 (8) (2017) 1373–1394, https://doi.org/10.1042/Bcj20160851.
[12] A. Moretton, S. Kourtis, A. Ganez Zapater, C. Calabro, M.L. Espinar Calvo, F. Fontaine, et al., A metabolic map of the DNA damage response identifies PRDX1 in the control of nuclear ROS scavenging and aspartate availability, Mol. Syst. Biol. 19 (7) (2023) e11267, https://doi.org/10.15252/msb.202211267.
[13] W. Ahmed, J. Lingner, PRDX1 counteracts catastrophic telomeric cleavage events that are triggered by DNA repair activities post oxidative damage, Cell Rep. 33 (5) (2020) 108347, https://doi.org/10.1016/j.celrep.2020.108347.
[14] V. Sharma, S. Bandyopadhyay, K. Sikka, A. Kakkar, G. Hariprasad, S.B. Singh, Label-free proteomics of oral mucosa tissue to identify potential biomarkers that can flag predilection of precancerous lesions to oral cell carcinoma: a preliminary study, Dis. Markers 2023 (2023) 1329061, https://doi.org/10.1155/2023/1329061.
[15] M. Bajor, A. Graczyk-Jarzynka, K. Marhelava, M. Kurkowiak, A. Rahman, C. Aura, et al., Triple combination of ascorbate, menadione and the inhibition of peroxiredoxin-1 produces synergistic cytotoxic effects in triple-negative breast cancer cells, Antioxidants 9 (4) (2020), https://doi.org/10.3390/antiox9040320.
[16] Y. Song, H. Liu, C. Cui, X. Peng, C. Wang, X. Tian, et al., Silencing of peroxiredoxin 1 inhibits the proliferation of esophageal cancer cells and promotes apoptosis by inhibiting the activity of the PI3K/AKT pathway, Cancer Manag. Res. 11 (2019) 10883–10890, https://doi.org/10.2147/CMAR.S235317.
[17] P. Thapa, H. Jiang, N. Ding, Y. Hao, A. Alshahrani, Q. Wei, The role of peroxiredoxins in cancer development, Biology 12 (5) (2023), https://doi.org/10.3390/biology12050666.
[18] W. Niu, M. Zhang, H. Chen, C. Wang, N. Shi, X. Jing, et al., Peroxiredoxin 1 promotes invasion and migration by regulating epithelial-to-mesenchymal transition during oral carcinogenesis, Oncotarget 7 (30) (2016) 47042–47051, https://doi.org/10.18632/oncotarget.9705.
[19] M. Zhang, M. Hou, L. Ge, C. Miao, J. Zhang, X. Jing, et al., Induction of peroxiredoxin 1 by hypoxia regulates heme oxygenase-1 via NF-kappaB in oral cancer, PLoS One 9 (8) (2014) e105994, https://doi.org/10.1371/journal.pone.0105994.
[20] J. Zhang, X. Jing, W. Niu, M. Zhang, L. Ge, C. Miao, et al., Peroxiredoxin 1 has an anti-apoptotic role via apoptosis signal-regulating kinase 1 and p38 activation in mouse models with oral precancerous lesions, Oncol. Lett. 12 (1) (2016) 413–420, https://doi.org/10.3892/ol.2016.4659.
[21] L.E. Dow, Modeling disease in vivo with CRISPR/Cas9, Trends Mol. Med. 21 (10) (2015) 609–621, https://doi.org/10.1016/j.molmed.2015.07.006.
[22] W.C. Skarnes, B. Rosen, A.P. West, M. Koutsourakis, W. Bushell, V. Iyer, et al., A conditional knockout resource for the genome-wide study of mouse gene function, Nature 474 (7351) (2011) 337–342, https://doi.org/10.1038/nature10163.
[23] C.A. Neumann, D.S. Krause, C.V. Carman, S. Das, D.P. Dubey, J.L. Abraham, et al., Essential role for the peroxiredoxin Prdx1 in erythrocyte antioxidant defence and tumour suppression, Nature 424 (6948) (2003) 561–565, https://doi.org/10.1038/nature01819.
[24] Y.J. Lee, Knockout mouse models for peroxiredoxins, Antioxidants 9 (2) (2020), https://doi.org/10.3390/antiox9020182.
[25] Q. Liu, Y. Zhang, PRDX1 enhances cerebral ischemia-reperfusion injury through activation of TLR4-regulated inflammation and apoptosis, Biochem. Biophys. Res. Commun. 519 (3) (2019) 453–461, https://doi.org/10.1016/j.bbrc.2019.08.077.

[26] R. Yanagisawa, E. Warabi, K. Inoue, T. Yanagawa, E. Koike, T. Ichinose, et al., Peroxiredoxin I null mice exhibits reduced acute lung inflammation following ozone exposure, J. Biochem. 152 (6) (2012) 595–601, https://doi.org/10.1093/jb/mvs113.
[27] N. Kikuchi, Y. Ishii, Y. Morishima, Y. Yageta, N. Haraguchi, T. Yamadori, et al., Aggravation of bleomycin-induced pulmonary inflammation and fibrosis in mice lacking peroxiredoxin I, Am. J. Respir. Cell Mol. Biol. 45 (3) (2011) 600–609, https://doi.org/10.1165/rcmb.2010-0137OC.
[28] S.U. Kim, Y.H. Park, J.M. Kim, H.N. Sun, I.S. Song, S.M. Huang, et al., Dominant role of peroxiredoxin/JNK axis in stemness regulation during neurogenesis from embryonic stem cells, Stem Cell. 32 (4) (2014) 998–1011, https://doi.org/10.1002/stem.1593.
[29] Y.H. Park, H.S. Kim, J.H. Lee, S.A. Choi, J.M. Kim, G.T. Oh, et al., Peroxiredoxin I participates in the protection of reactive oxygen species-mediated cellular senescence, BMB Rep 50 (10) (2017) 528–533, https://doi.org/10.5483/bmbrep.2017.50.10.121.
[30] L. Huang, H. Xiao, X. Xie, F. Hu, F. Tang, S.B. Smith, et al., Generation of Sigmar1 conditional knockout mouse using CRISPR-Cas9 gene targeting, Genesis 60 (6–7) (2022) e23487, https://doi.org/10.1002/dvg.23487.
[31] H. Zhi, T. Kanaji, G. Fu, D.K. Newman, P.J. Newman, Generation of PECAM-1 (CD31) conditional knockout mice, Genesis 58 (2) (2020) e23346, https://doi.org/10.1002/dvg.23346.
[32] M. Hafner, J. Wenk, A. Nenci, M. Pasparakis, K. Scharffetter-Kochanek, N. Smyth, et al., Keratin 14 Cre transgenic mice authenticate keratin 14 as an oocyte-expressed protein, Genesis 38 (4) (2004) 176–181, https://doi.org/10.1002/gene.20016.
[33] X. Wang, S. Zinkel, K. Polonsky, E. Fuchs, Transgenic studies with a keratin promoter-driven growth hormone transgene: prospects for gene therapy, Proc. Natl. Acad. Sci. U.S.A. 94 (1) (1997) 219–226, https://doi.org/10.1073/pnas.94.1.219.
[34] V. Vasioukhin, L. Degenstein, B. Wise, E. Fuchs, The magical touch: genome targeting in epidermal stem cells induced by tamoxifen application to mouse skin, Proc. Natl. Acad. Sci. U.S.A. 96 (15) (1999) 8551–8556, https://doi.org/10.1073/pnas.96.15.8551.
[35] M. Pei, D. Han, K.Y. Kim, D.W. Kim, W. Nam, H.J. Kim, et al., Risk factors of microscopically tumor-free surgical margins for recurrence and survival of oral squamous cell carcinoma patients, Front. Oncol. 12 (2022) 930988, https://doi.org/10.3389/fonc.2022.930988.